HOKKAIDO UNIVERSITY

Title	Sedimentary membrane lipids recycled by deep-sea benthic archaea
Author(s)	Takano, Yoshinori; Chikaraishi, Yoshito; Ogawa, Nanako O. et al.
Citation	Nature Geoscience, 3(12), 858-861 https://doi.org/10.1038/ngeo983
Issue Date	2010-11
Doc URL	https://hdl.handle.net/2115/45753
Type	journal article
File Information	Takano_naturegeosci_SI_2010.pdf, Supplementary Information

Supplementary Information (SI)

Sedimentary membrane lipids recycled by deep-sea benthic archaea

Yoshinori Takano[1*], Yoshito Chikaraishi[1], Nanako O. Ogawa[1], Hidetaka Nomaki[1],

Yuki Morono[2], Fumio Inagaki[2], Hiroshi Kitazato[1], Kai-Uwe Hinrichs[3]

& Naohiko Ohkouchi[1,4,5]

[1]*Institute of Biogeosciences, Japan Agency for Marine-Earth Science and Technology (JAMSTEC), 2-15 Natsushima, Yokosuka 237-0061, Japan.*

[2]*Kochi Institute for Core Sample Research, Japan Agency for Marine-Earth Science and Technology (JAMSTEC), Monobe B200, Nangoku, Kochi 783-8502, Japan.*

[3]*Department of Geosciences and MARUM Center for Marine Environmental Sciences, University of Bremen, D-28359, Bremen, Germany*

[4]*Department of Environmental Science and Technology, Tokyo Institute of Technology, 4259 Nagatsuda, Midori-ku, Yokohama, Kanagawa 226-8502, Japan*

[5]*Department of Earth and Planetary Sciences, University of Tokyo, 7-3-1 Hongo, Tokyo 113-0033, Japan*

E-mail: takano@jamstec.go.jp; nohkouchi@jamstec.go.jp

Methods

1. Geological setting and *in situ* ^{13}C-tracer experiment at the sea-floor

In the present study, we conducted *in situ* ^{13}C-tracer experiments for 0–405 days based on I-K type incubation[17] and using the ROV *Hyper-Dolphin* and its mother research vessel the RV *Natsushima* at Sagami Bay[31-39], Japan (35˚00.8'N, 139˚21.6'E; cruises NT06-04,-05,-22 and NT08-02, Suppl. Fig. 1). In these experiments, we used ^{13}C-labeled glucose (^{13}C$_6$H$_{12}$O$_6$, 98.7 atom%; Cambridge Isotope Co. Ltd) as a ^{13}C-substrate. Approximately 600 ml of bottom water was present in the top of the culture cores. Sediments were sliced at 1-cm intervals from 0 to 5 cm in depth, followed by samples at sediment depths of 5–7, 7–10 and 10–15 cm. Subsamples (15 cm^3) of the sediments were used for analyses of bulk organic matter. The collected samples were stored at −80°C until use.

2. Measurement of carbon isotopic composition

2-1. Bulk isotope analysis and total organic carbon in the sediment

Dried sediment (*ca*. 2 mg) was transferred to pre-cleaned silver cups and decalcified using 2 M HCl followed by drying on a hotplate. Dried silver cups containing decalcified samples were sealed into pre-cleaned tin cups prior to isotopic analysis. Carbon isotopic composition and total organic carbon content were determined using an isotope ratio monitoring mass spectrometer (Delta V, Thermo Scientific) connected to an elemental analyser (Flash EA1112, CE Instruments). Carbon isotopic compositions are expressed using conventional δ notation ($\delta^{13}C = [(^{13}C/^{12}C)_{sample} / (^{13}C/^{12}C)_{standard} − 1] \times 1000$).
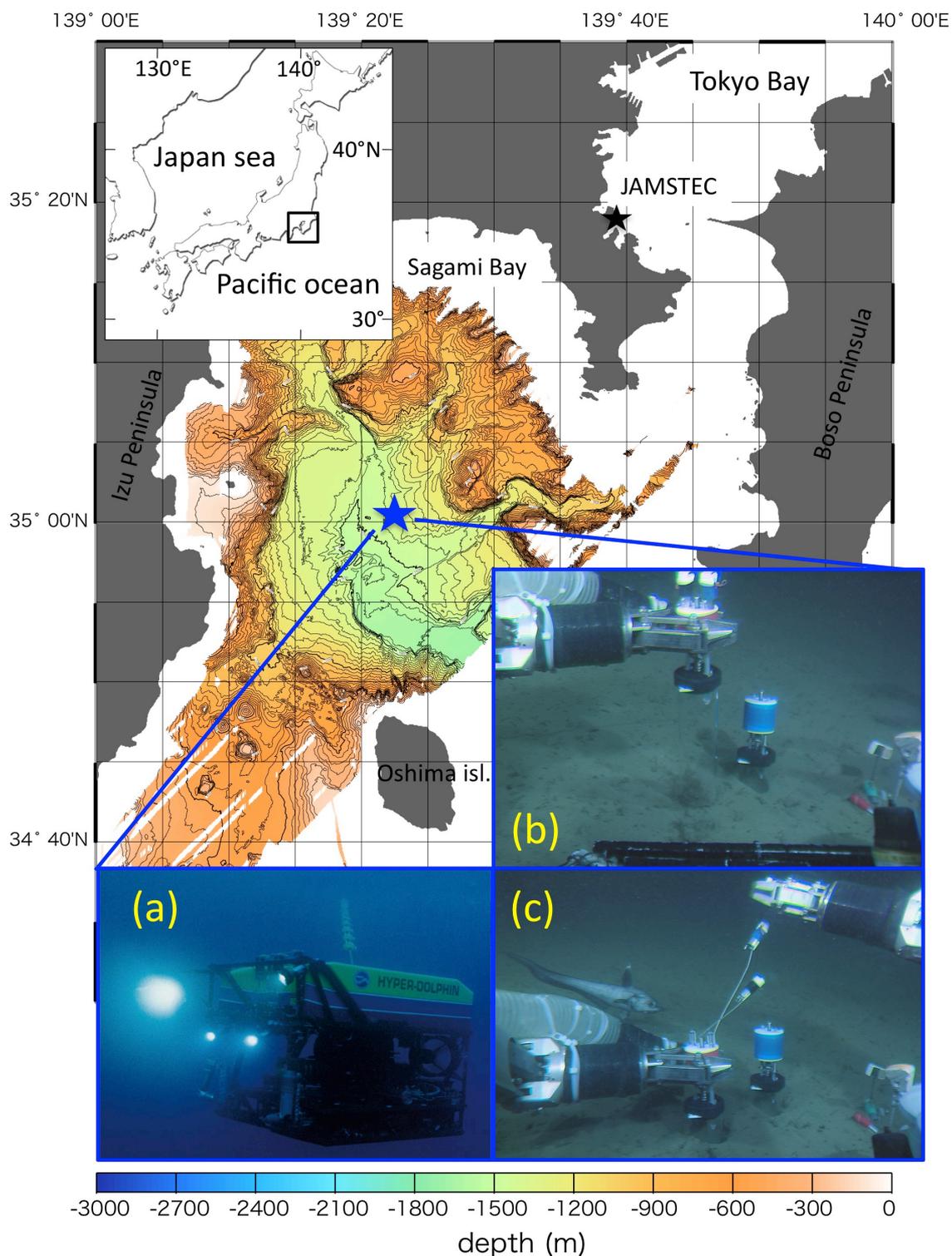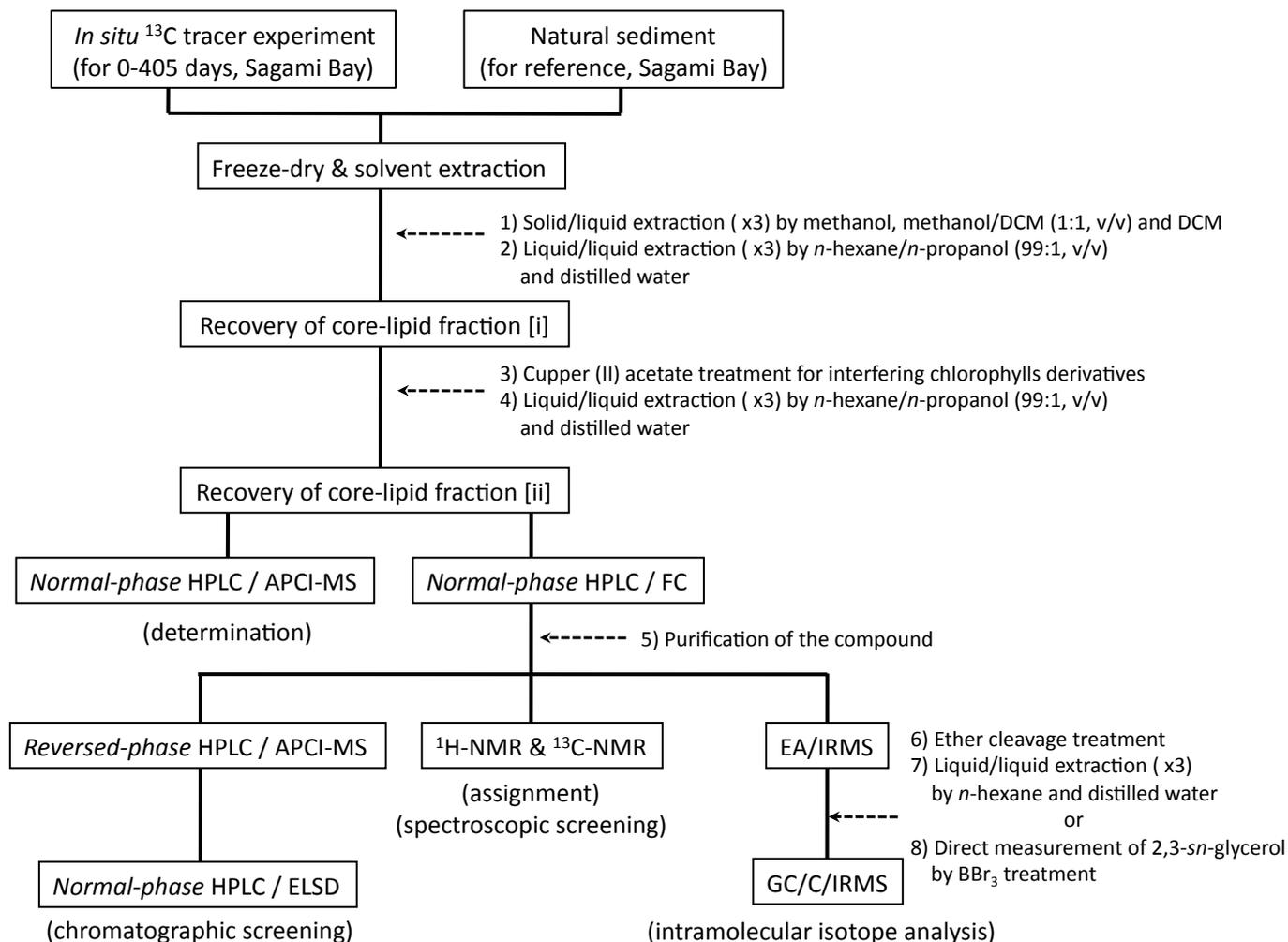
Supplementary Figure 1.

Geological location and bathymetric chart of the *in situ* ^{13}C-experiments in a deep-sea environment in Sagami Bay, Western Pacific[40]. **a**, the remotely operated vehicle *Hyper-Dolphin*. **b**, **c**, *in situ* incubation chamber for the experiment by during cruise NT06-04&05, NT08-02.

```
┌─────────────────────────────┐   ┌─────────────────────────────┐
│ In situ ¹³C tracer experiment│   │     Natural sediment        │
│ (for 0-405 days, Sagami Bay) │   │ (for reference, Sagami Bay) │
└─────────────────────────────┘   └─────────────────────────────┘
```

Freeze-dry & solvent extraction

1) Solid/liquid extraction (x3) by methanol, methanol/DCM (1:1, v/v) and DCM
2) Liquid/liquid extraction (x3) by *n*-hexane/*n*-propanol (99:1, v/v)
   and distilled water

Recovery of core-lipid fraction [i]

3) Cupper (II) acetate treatment for interfering chlorophylls derivatives
4) Liquid/liquid extraction (x3) by *n*-hexane/*n*-propanol (99:1, v/v)
   and distilled water

Recovery of core-lipid fraction [ii]

Normal-phase HPLC / APCI-MS

(determination)

Normal-phase HPLC / FC

5) Purification of the compound

Reversed-phase HPLC / APCI-MS

¹H-NMR & ¹³C-NMR

(assignment)
(spectroscopic screening)

EA/IRMS

6) Ether cleavage treatment
7) Liquid/liquid extraction (x3)
   by *n*-hexane and distilled water
   or
8) Direct measurement of 2,3-*sn*-glycerol
   by BBr_3 treatment

Normal-phase HPLC / ELSD

(chromatographic screening)

GC/C/IRMS

(intramolecular isotope analysis)

Supplementary Figure 2.

Experimental procedures employed in the extraction, separation and purification for compound-specific carbon isotopic analysis (CSIA) and intramolecular carbon isotopic analysis.

2-2. Compound-specific isotope analysis (CSIA) of caldarchaeol and crenarchaeol

We determined the archaeal core lipids of caldarchaeol and crenarchaeol derived mainly from *Euryarchaeota* and *Crenarchaeota*[41-44]. Freeze-dried sediments (ca. 1–5 g) were extracted by ultra-sonication (20 min) and centrifuged (2,000 rpm, 5 min) three times with methanol, three times with dichloromethane (DCM)/methanol (1:1, v/v) and three times with DCM during solid/liquid extraction (Suppl. Fig. 2). All the extracts were combined and then dried under a nitrogen flow. Five mL distilled water and 5 mL *n*-hexane/*n*-propanol (99:1, v/v) were added and samples were shaken for 1 min for liquid/liquid extraction three times. The recovered *n*-hexane/*n*-propanol (99:1, v/v) was then dried under a nitrogen flow. To eliminate chlorophyll derivatives potentially interfere with crenarchaeol during purification, 5 mL of saturated copper acetate dissolved in acetone was added and kept overnight.

Saturated copper acetate in acetone was dried under a nitrogen flow, and then 5 mL distilled water and 5 mL *n*-hexane/*n*-propanol (99:1, v/v) were added and samples were shaken for 1 min for liquid/liquid extraction three times. The recovered *n*-hexane/*n*-propanol (99:1, v/v) was then dried and dissolved in 2 mL *n*-hexane/*n*-propanol (99:1, v/v). Using HPLC/APCI-MS, the recovered tetraether core lipids were eluted isocratically with 99% *n*-hexane and 1% *n*-propanol for 5 min, followed by a linear gradient to 1.8% *n*-propanol with a flow rate of 0.2 mL min^{-1}. Separation was achieved on a Prevail Cyano (2.1 × 150 mm, 3 μm; Alltech, Deerfield, IL) fitted with the same packing guard column (4 × 7.5 mm;) [45]. Occasionally, we used internal standard (C_{46}GDGT) to determine the concentration of extractable GDGTs[45].
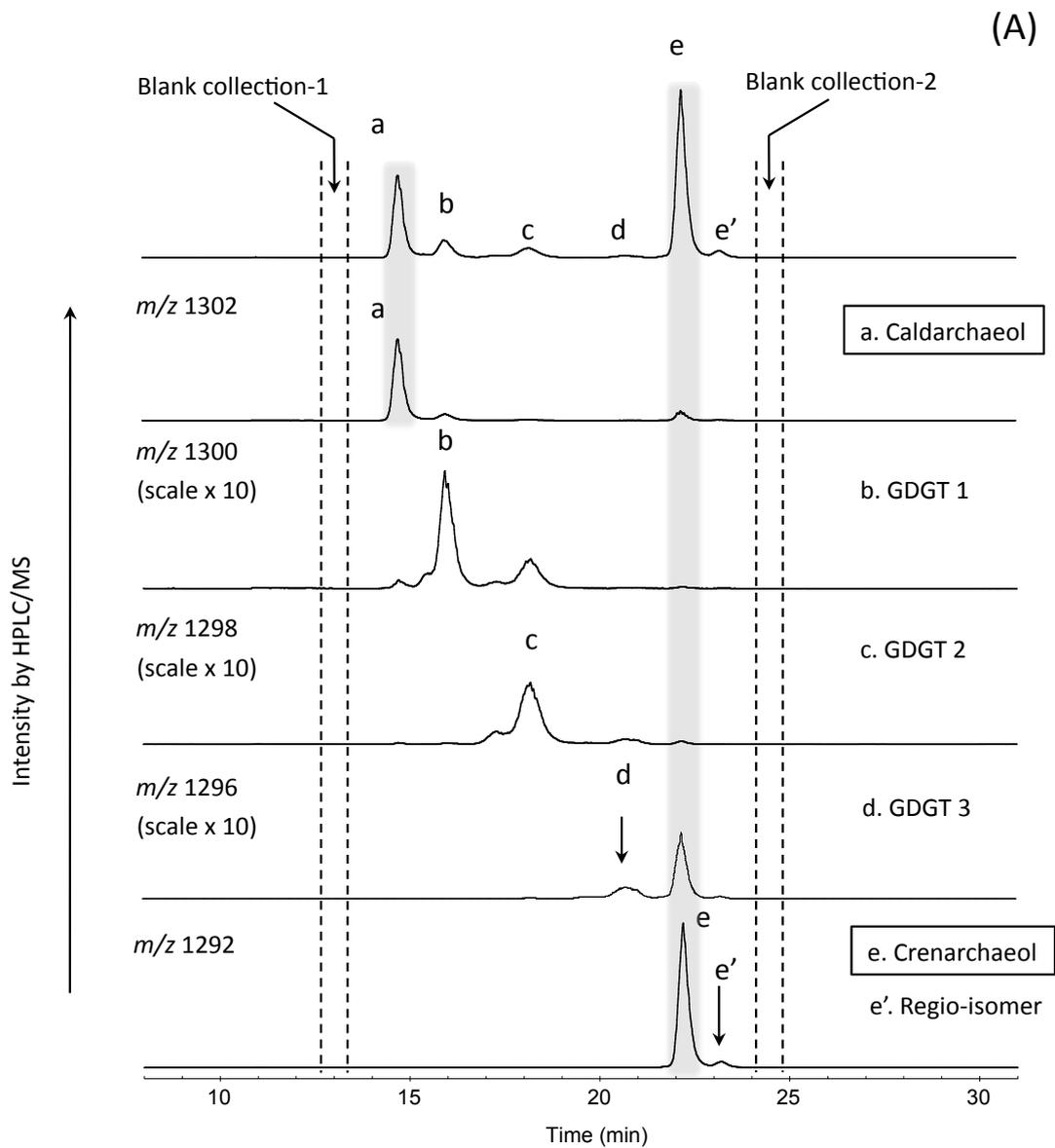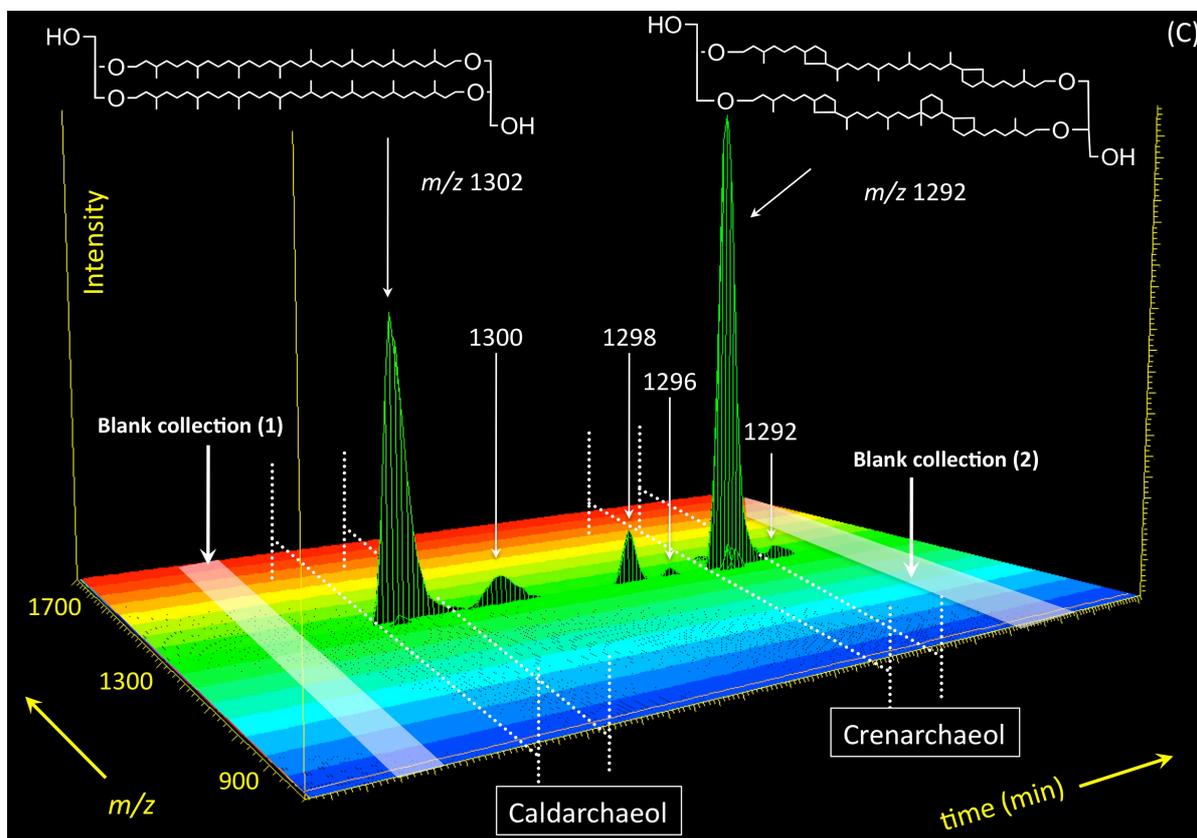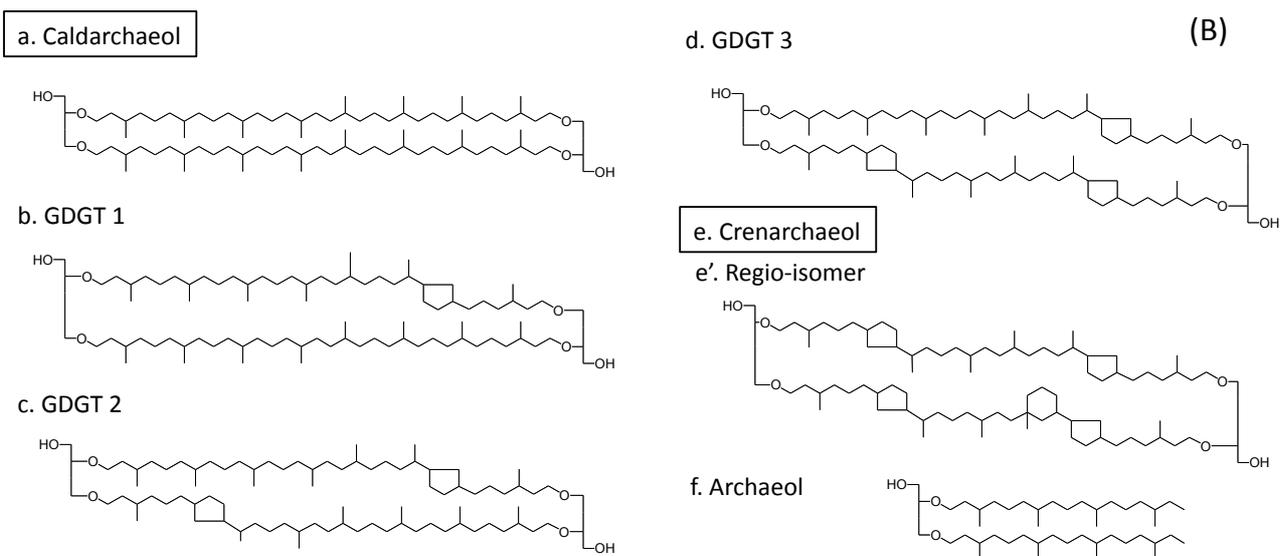
Supplementary Figure 3.

Determination of caldarchaeol and crenarchaeol by HPLC/APCI-MS.

(A) Representative chromatogram of archaeal tetraether lipids obtained from deep-sea sediment (natural reference sample) at Sagami Bay.

a. Caldarchaeol

b. GDGT 1

c. GDGT 2

d. GDGT 3

e. Crenarchaeol
e'. Regio-isomer

f. Archaeol

(B)

(C)

m/z 1302

1300

1298
1296

m/z 1292

1292

Intensity

Blank collection (1)

Blank collection (2)

Crenarchaeol

Caldarchaeol

1700

1300

900

m/z

time (min)

Supplementary Figure 3.

(B) Structures of GDGTs along with the corresponding mass chromatograms. Archaeol was under detection limit. (C) Three-dimensional plot (retention time, *m/z* and its abundance) of GDGTs from deep-sea sediment (natural reference sample) at Sagami Bay.

The guard column and main column were maintained at 40°C in a column oven with pre-heating chamber for eluent inlet (Polaratherm). Great care was taken to ensure consistent retention times for each compound, as described above. Detection was achieved using atmospheric-pressure positive ion chemical ionization mass spectrometry (APCI-MS). Conditions for APCI-MS were as follows: nebulizer pressure 60 psi, vaporizer temperature 300°C, drying gas (N_2) flow 6 L/min and temperature 250°C, and corona 5 mA (3.2 kV). Positive ion spectra were generated by scanning selected ion monitoring (SIM) and total scanning of *m/z* 500–1500 to monitor the base-line resolution (Suppl. Fig. 3-A). Although we verified the detection of extractable archaeol (diether lipid of Archaea) using cultured *Methanobacterium* sp., the amount was not significant in the sediment samples collected from Sagami Bay.

In order to check the purity of those "isolated" compounds from G-0, G-9, and G-405 samples, we conducted additional screening analyses with reversed-phase (RP) HPLC/APCI-MS, HPLC combined with an evaporative light scattering detector (ELSD) and ^{1}H-, ^{13}C-NMR.

> **RP-HPLC/APCI-MS:** Firstly, for a screening analysis of the purified compound by RP-HPLC/APCI-MS, the purified compound was eluted isocratically with 100% methanol and 0% acetone for 0 min, followed by a linear gradient to 100% acetone till 45 min with a flow rate of 0.5 mL min^{-1}. Separation was achieved on a Zorbax SB-C18 SSP (3.0 × 150 mm, 3.5 μm; Agilent) fitted with the same packing guard column (4 × 7.5 mm). The guard column and main column were

maintained at 40°C in a column oven with pre-heating chamber for eluent inlet (Polaratherm). Detection was achieved using APCI-MS. Conditions for APCI-MS were: nebulizer pressure 60 psi, vaporizer temperature 300°C, drying gas (N_2) flow 6 L/min and temperature 250°C, and corona 5 mA (3.2 kV). Positive ion spectra were generated by total ion scanning of *m/z* 100–2000 (Suppl. Fig. 3-D). We detected single compound peak showing caldarchaeol or crenarchaeol in the chromatogram. Furthermore, the fragment ion was also assigned each purified compound.

HPLC/ELSD: Secondly, to authenticate this screening analysis more carefully with the ELSD (PL-ELS2100, Polymer Laboratories Ltd), the HPLC condition was same as abovementioned normal-phase HPLC. Conditions for ELSD were as follows: evaporator temperature 30°C, nebulizer temperature 30°C, and drying air gas flow 1.60 SLM. The advantage of HPLC/ELSD is that we can detect any compound regardless of its molecular weight or ionization efficiency (Suppl. Fig. 3-E). Here, we detected a single peak of each compound by ELSD. Hence, we concluded that there is no significant co-extracted/co-eluted hidden contaminants including hidden small compounds.

^{1}H- and ^{13}C-NMR: Thirdly, to determine the identity of purified caldarchaeol and crenarchaeol, aliquots of the purified compounds (4-5 μg) were dissolved in 50 μL of $CDCl_3$ (>99%) in a 1 mm probe and subsequently analyzed by ^{1}H-NMR (400

MHz, Bruker Biospin). We also analyzed by ^{13}C-NMR by 5 mm probe to verify its purity and possible any ^{13}C-contaminants. The pulse programs we used were composite pulse decoupling for precise ^{13}C-chemical shift assignment (C13CPD) and inverse gate decoupling for precise ^{13}C-quantitative determination (C13IG) by full scan range chemical shift. The advantage of NMR over chromatographic screenings is that we can detect any dissolved contaminants on the full range chemical shift. Although ^{13}C-NMR scanned purified caldarchaeol and crenarchaeol, we only detected $CHCl_3$ (solvent: $CDCl_3$, locking to ^{1}H-/^{13}C-NMR). Our sample size (4-5 µg) was more than 2 orders of magnitude smaller than that required for the structure assignment by ^{13}C-NMR [e.g., 44]. Note that the isotopic analysis of glycerol resulted in direct evidence for selective ^{13}C incorporation in this molecular moiety. Contamination compounds were not detected in both ^{1}H-&^{13}C-NMR analysis. Simultaneously, we conducted structure assignment for the purified compound by ^{1}H-NMR (Suppl. Fig. 3-F, G). Overall, we concluded purity of caldarchaeol and crenarchaeol were high enough to avoid interference of "^{13}C-contaminants".
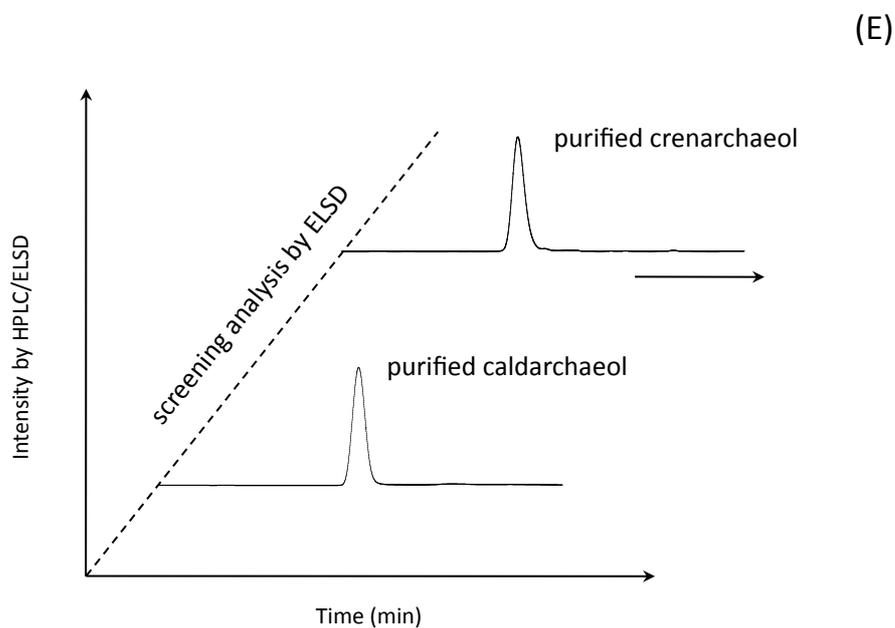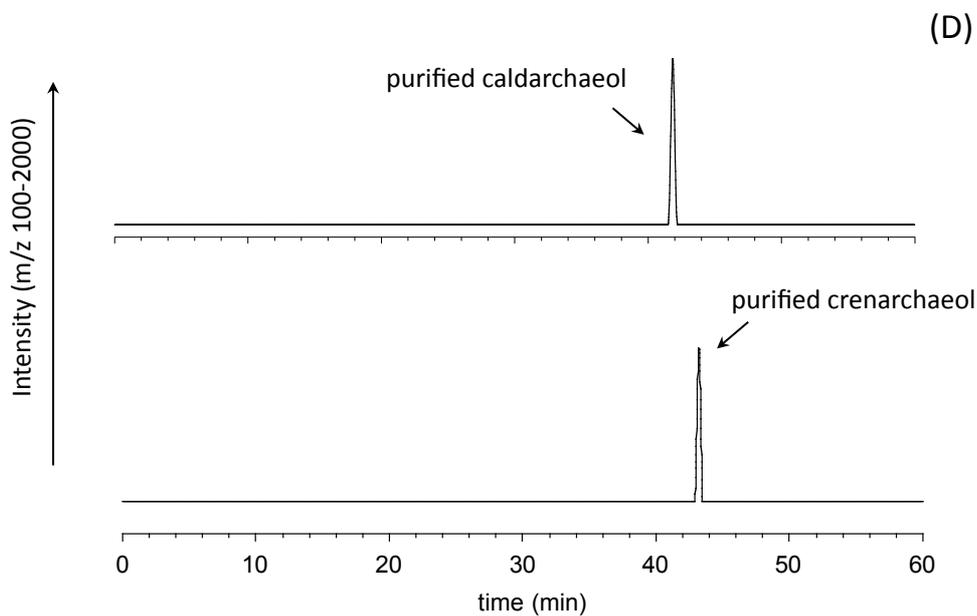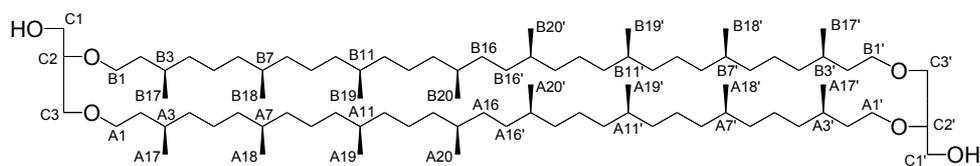
Supplementary Figure 3.

(D) Screening analysis for the "purified fractions" of caldarchaeol and crenarchaeol from G-0, G-9, and G-405 samples by using RP-HPLC/APCI-MS. (E) Screening analysis by using HPLC/ELSD.
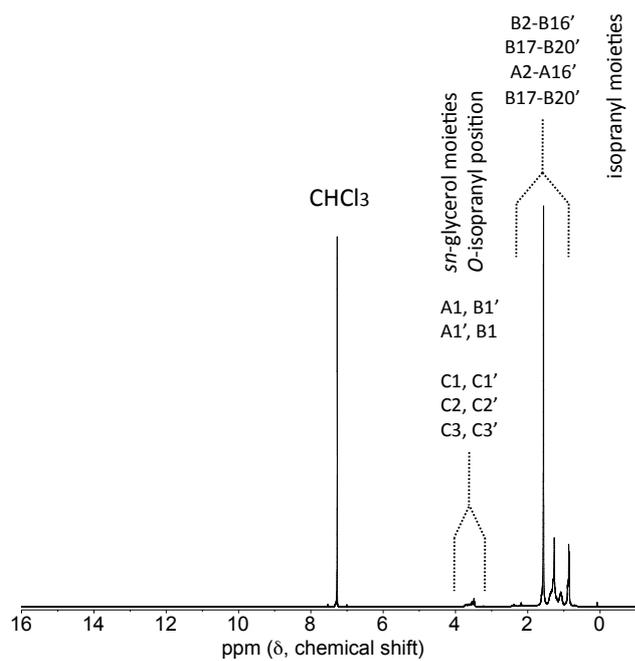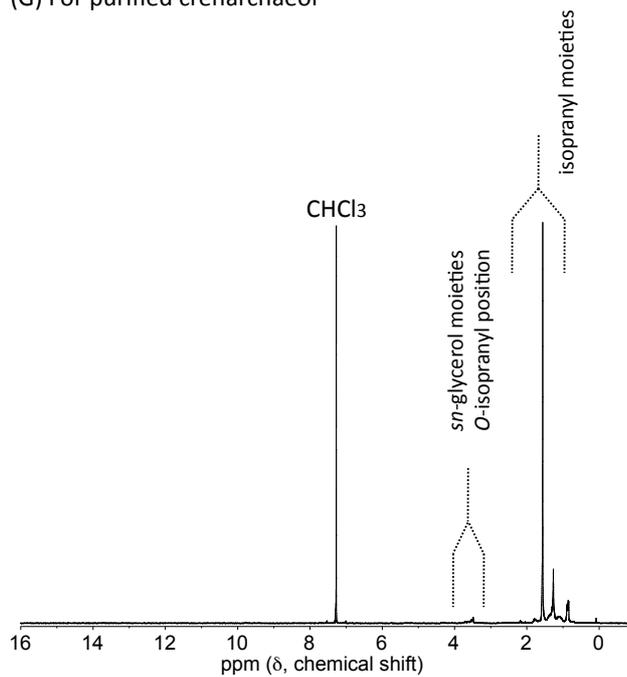
The structure of component for glycerol dibiphytanyl glycerol tetraether (*e.g.*, caldarchaeol)

(F) ^{1}H-NMR for purified caldarchaeol

(G) For purified crenarchaeol

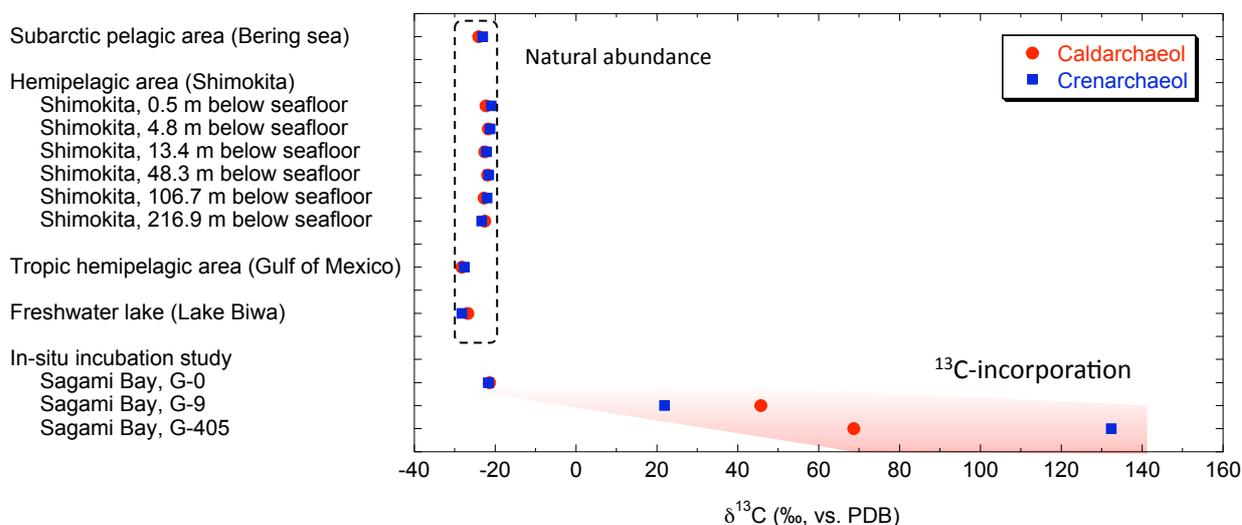**Supplementary Figure 3.**

(F, G) Screening analysis by using ^{1}H-NMR.

The carbon isotopic compositions of the purified caldarchaeol and crenarchaeol were determined using a ThermoFinnigan Delta Plus XP coupled with an EA1112 via a Conflo III interface[46,47]. Compared with the natural ^{13}C-abundances of caldarchaeol and crenarchaeol in various sediment samples, we could clearly recognize the distinct carbon isotopic compositions of the experimental blank (G-0) and the long-term *in situ* incubations (G-9, G-405) at Sagami Bay (Suppl. Fig. 4). The most abundant tetraethers were caldarchaeol and crenarchaeol on the whole; GDGT 1, GDGT2 and GDGT3 represented minor components.

Supplementary Figure 4.

Comparison of $\delta^{13}C_{caldarchaeol}$ and $\delta^{13}C_{crenarchaeol}$ from various locations[71-73] and *in situ* ^{13}C-tracer samples. Sample courtesy from T. Toyofuku (JAMSTEC) for Bering sea sediment (KH97-2 cruise).

2-3. Carbon isotopic compositions of biphytanes (BP) and 2,3-*sn*-glycerol in tetraethers

To analyze the biphytanes of caldarchaeol and crenarchaeol, we performed an ether cleavage treatment using an improved method described in the literature[27,28]. Briefly, a portion of the caldarchaeol and crenarchaeol purified by the abovementioned HPLC procedure was dried under a gentle nitrogen flow and then refluxed in 1 mL of 57 wt% HI (in H_2O) in 16 × 100 mm reaction vials with PTFE-lined caps at 110°C for 4 hr. After 5 mL of 5 wt% NaCl aqueous solution and 5 mL *n*-hexane were added, *n*-hexane fraction was recovered by three times liquid/liquid extraction. Five mL *n*-hexane and 5 mg PtO_2 were added to the sample in a test tube, and hydrogenation was carried out by gentle H_2 gas bubbling at room temperature for 30 min. Finally, the *n*-hexane fraction was recovered again. We determined carbon isotopic compositions for each isoprenoid (BP[0], BP[2], and BP[3]) using GC/C/IRMS, resulting in the determination of carbon isotopic compositions for 2,3-*sn*-glycerol ($\delta^{13}C_{2,3\text{-}sn\text{-glycerol}}$) using the mass balance equation between $\delta^{13}C_{CSIA}$ and its intramolecular $\delta^{13}C_{BP}$ (Suppl. Figs. 5&6). Theoretically, the mass balance equation takes the form

$$n_X \delta^{13}C_X = n_Y \delta^{13}C_Y + n_Z \delta^{13}C_Z$$

where *n* is the number of moles of carbon, resulting in $n_X = n_Y + n_Z$. The subscripts *X*, *Y* and *Z* represent whole-molecule compounds, a specific group, and a second specific group, respectively. Hence, the 86 comes from carbon number of caldarchaeol and crenarchaeaol (*i.e.*, $C_{86}H_{172}O_6$ and $C_{86}H_{162}O_6$, respectively).

The employed GC/C/IRMS system was a ThermoFinnigan Delta Plus XP combined with an Agilent 6890N GC and an Ultra-2 capillary column (5% phenyl, 95% methyl polysiloxane; 25 m × 0.32 mm i.d., 0.52 μm film thickness; Agilent). The GC oven temperature was programmed as follows: an initial temperature of 40°C, ramped up at 30°C min^{-1} to 120°C, and then ramped up at 6°C min^{-1} to 320°C, where it was maintained for 20 min. The analytical precision (1σ) was better than 0.3‰, as determined by repeated injections of a mixture of *n*-alkane standards[64].

Sample: Shimokita, 48.2m (sec 6-3), compound: caldarchaeol

CSIA by EA/IRMS

$\delta^{13}C_{caldarchaeol}$= -21.9 ‰

ether cleavage

Intra-molecular CSIA by GC/C/IRMS

$\delta^{13}C_{biphytan[0]}$ = -20.9 ‰

Total ion chromatogram by GC/MS

intensity

Time (min)

+ x 2

$\delta^{13}C_{2,3\text{-}sn\text{-glycerol}}$= -34.9 ± 6 ‰
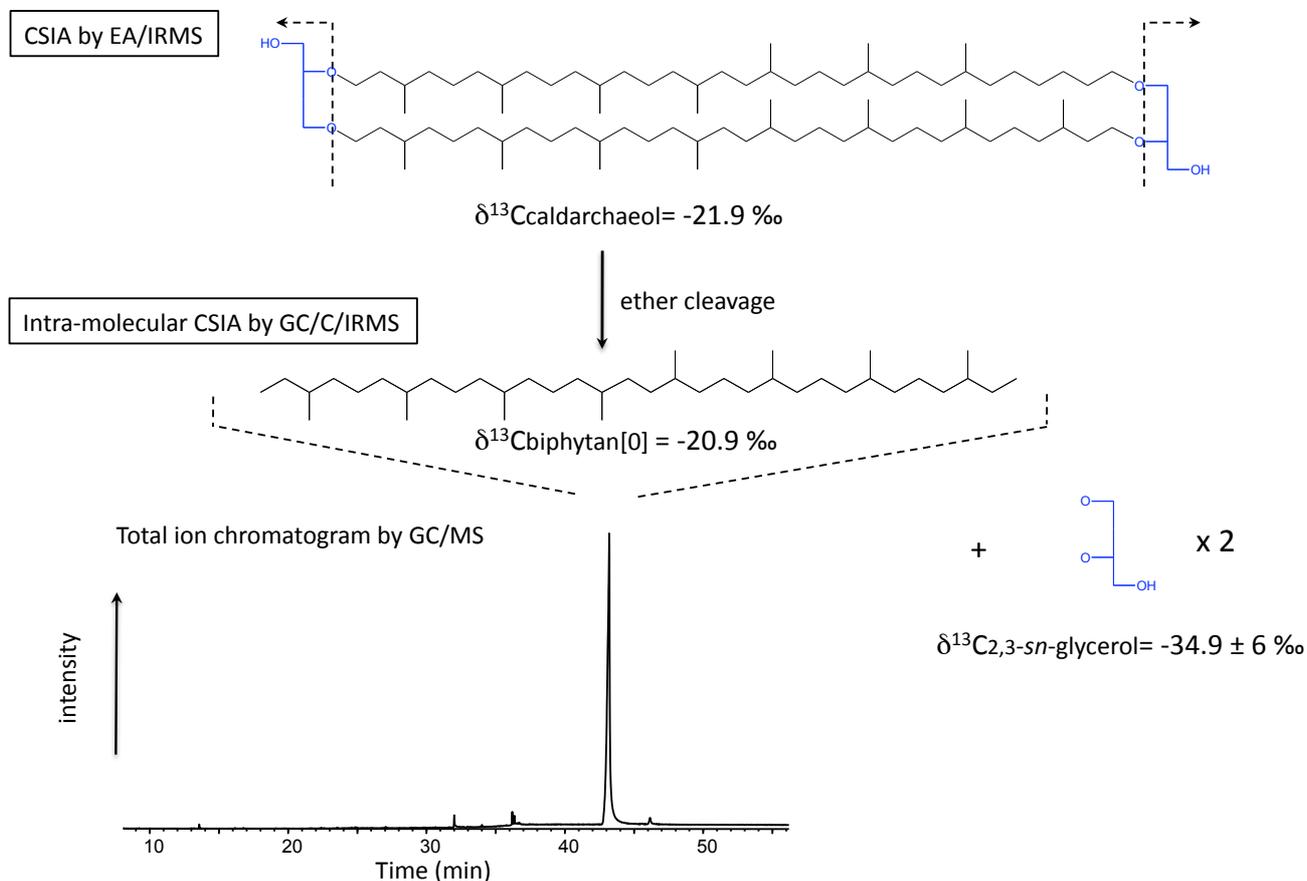
Supplementary Figure 5.

Preliminary verification of the present compound-specific isotope analysis (CSIA) and intramolecular isotopic analysis. Here, the marine sediment was collected from off-shore Shimokita, Japan, Western Pacific (CK06-06, section 6-3; depth, 48.2 m below the sea-floor)[71]. As seen in the GC/MS chromatogram, the HPLC-purified caldarchaeol did not contain other core lipid compounds, resulting in a single peak of BP [0] being detected in the purified fraction.

Sample: Sagami Bay, G-405, 0-1cm, compound: caldarchaeol & crenarchaeol

CSIA by EA/IRMS

ether cleavage

ether cleavage

$\delta^{13}C_{caldarchaeol} = + 68.7 ‰$

ether cleavage treatment

Intra-molecular CSIA by GC/C/IRMS

x 2

$\delta^{13}C_{BP[0]} = -22.0 ‰$

+
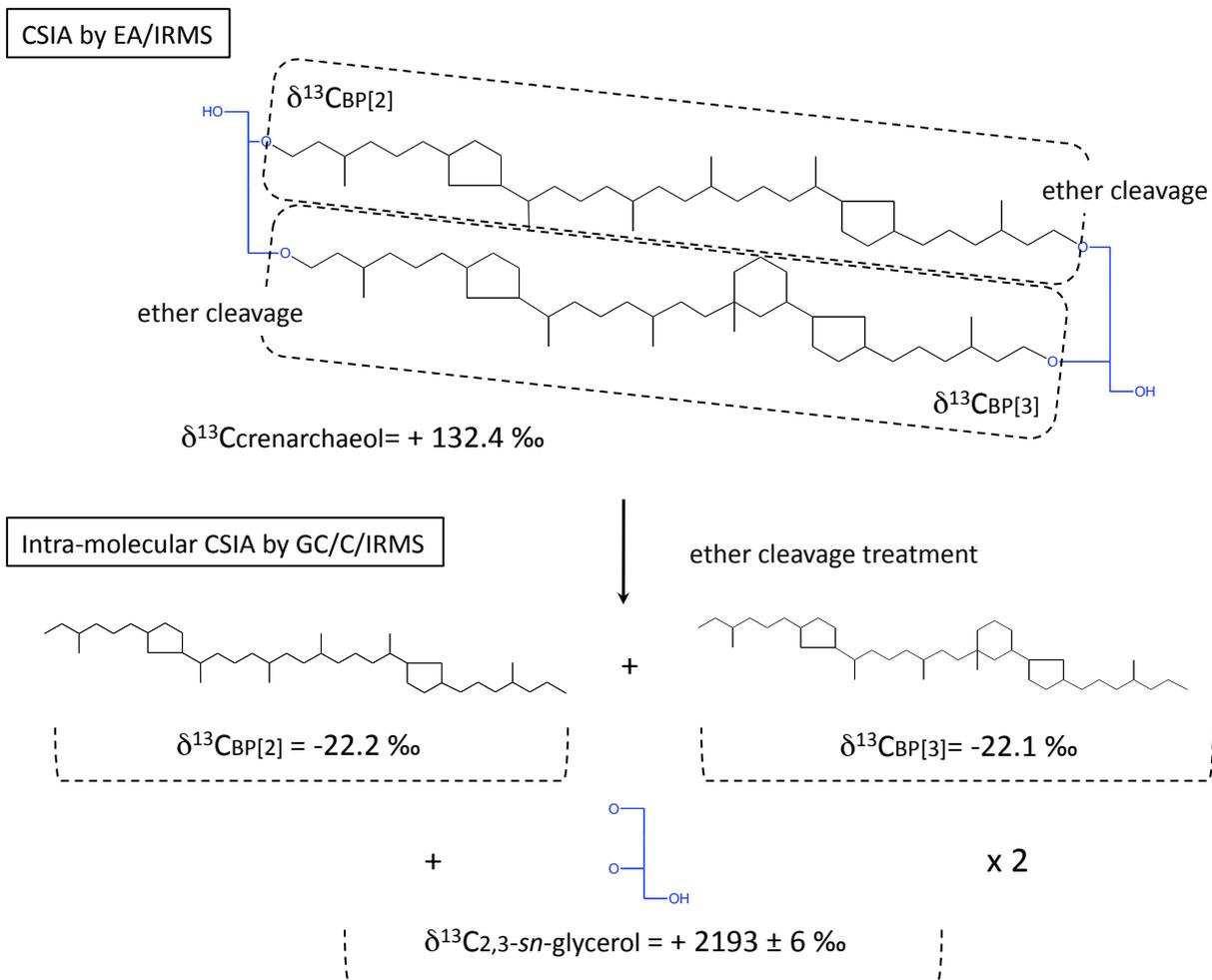
x 2

$\delta^{13}C_{2,3\text{-}sn\text{-glycerol}} = + 1278 ± 6 ‰$
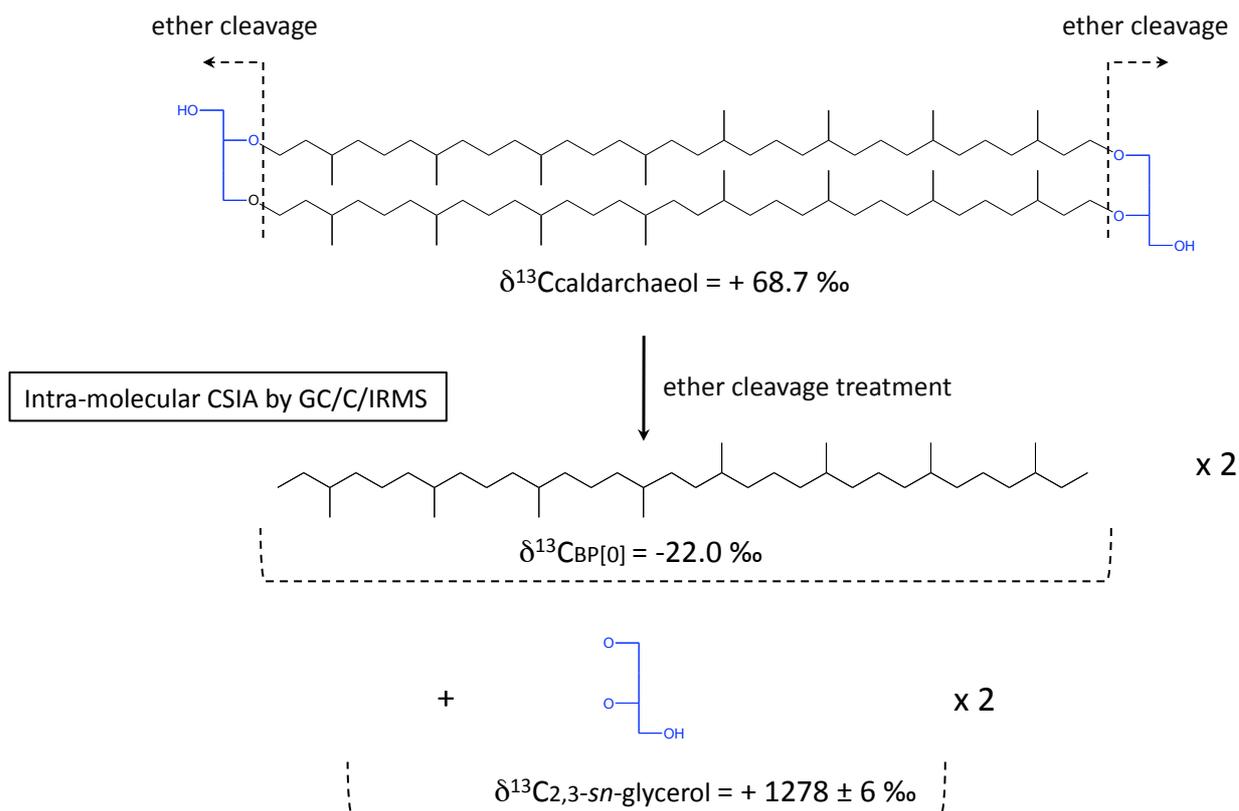
Supplementary Figure 6.

Molecular structure and carbon isotopic compositions CSIA after 405 days of the *in situ* ^{13}C-tracer experiment at Sagami Bay. Although the present *in situ* tracer experiments do not provide any information concerning energy sources or the energetic balance[25] of biological activity with respect to the growth (cell replication), maintenance (sustained activity) and survival (retained viability) of benthic *Euryarchaeota* and *Crenarchaeota*, we are able to estimate metabolic intensity during archaeal lipid synthesis of 2,3-*sn*-glycerol and isoprenoids (see also Suppl. Figure 7).

Sample: Sagami Bay, G-405, 0-1cm, compound: caldarchaeol & crenarchaeol

CSIA by EA/IRMS

$\delta^{13}C_{BP[2]}$

HO

ether cleavage

ether cleavage

$\delta^{13}C_{BP[3]}$

OH

$\delta^{13}C_{crenarchaeol} = + 132.4 ‰$

Intra-molecular CSIA by GC/C/IRMS

ether cleavage treatment

$\delta^{13}C_{BP[2]} = -22.2 ‰$

$+$

$\delta^{13}C_{BP[3]} = -22.1 ‰$

$+$

OH

x 2

$\delta^{13}C_{2,3\text{-}sn\text{-glycerol}} = + 2193 \pm 6 ‰$

Supplementary Figure 6.

(Continued from previous page)

3. Direct measurement of 2,3-*sn*-glycerol moieties by online GC/C/IRMS

For further confirmation of the mass balance estimation regards to ^{13}C-enriched glycerol, we have successfully determined the carbon isotopic composition of 2,3-*sn*-glycerol derivatives derived from caldarchaeol and crenarchaeol with GC/C/IRMS. The purified compound (*i.e.*, caldarchaeol or crenarchaeol) in 5 ml reaction vial were dried under gentle nitrogen flow. We added 0.5 ml of DCM and 50 µl of 1.0 M boron tribromide (BBr$_3$, Wako chemical) to each sample and put the sample in the heat block at 60°C for 2 hours. After cooling down, we added 0.5 ml of distilled water to stop the reaction. We did a liquid/liquid extraction by adding 1 ml of DCM and collected the DCM fraction in three times. After dryness of the DCM fraction by gentle nitrogen flow in hot sand bath (< 80°C), the final fraction containing glycerol bromide-derivatives were re-dissolved by 50 µl of DCM. The employed GC/C/IRMS system was a ThermoFinnigan Delta Plus XP combined with an Agilent 6890N GC and an HP-1MS capillary column (30 m × 0.25 mm i.d., 0.1 µm film thickness; Agilent). GC separation conditions of 2,3-*sn*-glycerol derivatives were optimized by 1,2,3-tribromopropane standard (C$_3$H$_5$Br$_3$, Aldrich) in DCM. The GC oven temperature was programmed as follows: an initial temperature of 50°C, ramped up at 50°C min^{-1} to 260°C.

The carbon isotopic composition of glycerol moieties in G-405 samples for the purified caldarchaeol and crenarchaeol were up to +1900‰ and +2780‰, respectively. Consequently, the mass balance estimation is consistent with present direct measurement of 2,3-*sn*-glycerol moieties. Our data is novel findings in terms of the evidence for intramolecular large disparity during benthic archaeal heterotrophic processes.

4. Carbon isotopic composition of dissolved inorganic carbon (DIC) in head-space water

As to onboard treatment for $\delta^{13}C_{DIC}$, three 20 ml bottles of overlying water samples were gently collected from all cores to determine ^{13}C concentrations in dissolved inorganic carbon (DIC). Soon after their collection, the seawater samples were poisoned with $HgCl_2$, sealed with rubber septum-aluminum cap and then preserved at 4°C prior to analyses. In the on-shore laboratory, 3 ml of the bottled overlying seawater was mixed with 0.5 ml of pure H_3PO_4 in a vacuumed chamber to extract dissolved CO_2 gas in the seawater. The liberated CO_2 was purified through repeated freezing and thawing. The carbon isotopic ratio of the purified CO_2 was measured by a stable isotope mass spectrometer (GV Instruments, IsoPrime). Standard CO_2 gas was used as a working standard. The overall precision of $\delta^{13}C$ analyses is ~0.1‰ based on analyses of different aliquots of a seawater sample. In a case when ^{13}C concentration was too high (i.e. >~100‰), the seawater sample was proportionally (typically 1:10) mixed with surface seawater that have known isotopic value. The carbon isotopic composition of original seawater was calculated from mass balance equation of measured sample and added surface seawater samples. Those dilution samples were prepared as duplicate or triplicate samples independently to ensure the accuracy of the measurements.

## 5. Peculiar ^{13}C-isoprenoid behavior: implications of recycling processes from outer membrane in Prokaryotes

Biosynthesis pathway of core lipids in Archaea for isoprenoid and 2,3-*sn*-glycerol moieties were shown in Suppl. Fig. 7. The metabolic intensity of the glycolytic pathways, referred to as the EM and ED pathways, was more pronounced than that in the mevalonate (MVA) and modified MVA pathways to produce isoprenoid alkyl chains. Following the production of DGGGP, several steps are required to form tetraether lipids: (1) saturation of isoprenyl chains, (2) head-to-head condensation to form the tetraether core moiety, and (3) modification of a polar group from a simple phosphate group to a sugar and/or a modified phosphoric ester group. The order of these steps remains unclear. The enzymes involved in ether bond formation and cytidine 5'-diphosphate (CDP) addition require the fully unsaturated form of the C_{20} isopranyl alcohol[67,68]. Hence, the saturation of double bonds is expected to occur following CDP addition to DGGGP[69]. However, mechanisms of head-to-head linkage reactions of tetraether lipid synthesis are not confirmed and have been the topic of lengthy discussion even in the laboratory tracer experiment[69,76]. Conclusion of Zhang and Poulter (1993) was based on *in vitro* studies of halophilic and thermophilic archaea under nutrient-enriched environments[68]. Nicolaus et al. (1990) also reported uneven ^{14}C- and ^{3}H- incorporation to cultured archaeal lipids by thermophilic *Sulfolobus solfataricus*[74]. It is important to note that our study is concerning about deep-sea cosmopolitan species under starving condition. In heterotrophic archaea, exogenously supplied glycerol is incorporated and phosphorylated by ATP *via* the catabolic pathway[70]. Ohnuma et al. (1996) reported that a salvage pathway for polyprenols was detected in *Sulfolobus acidocaldarius*, in which geranylgeraniol and geranylgeranyl monophosphate were phosphorylated with ATP by separate enzymes[75].
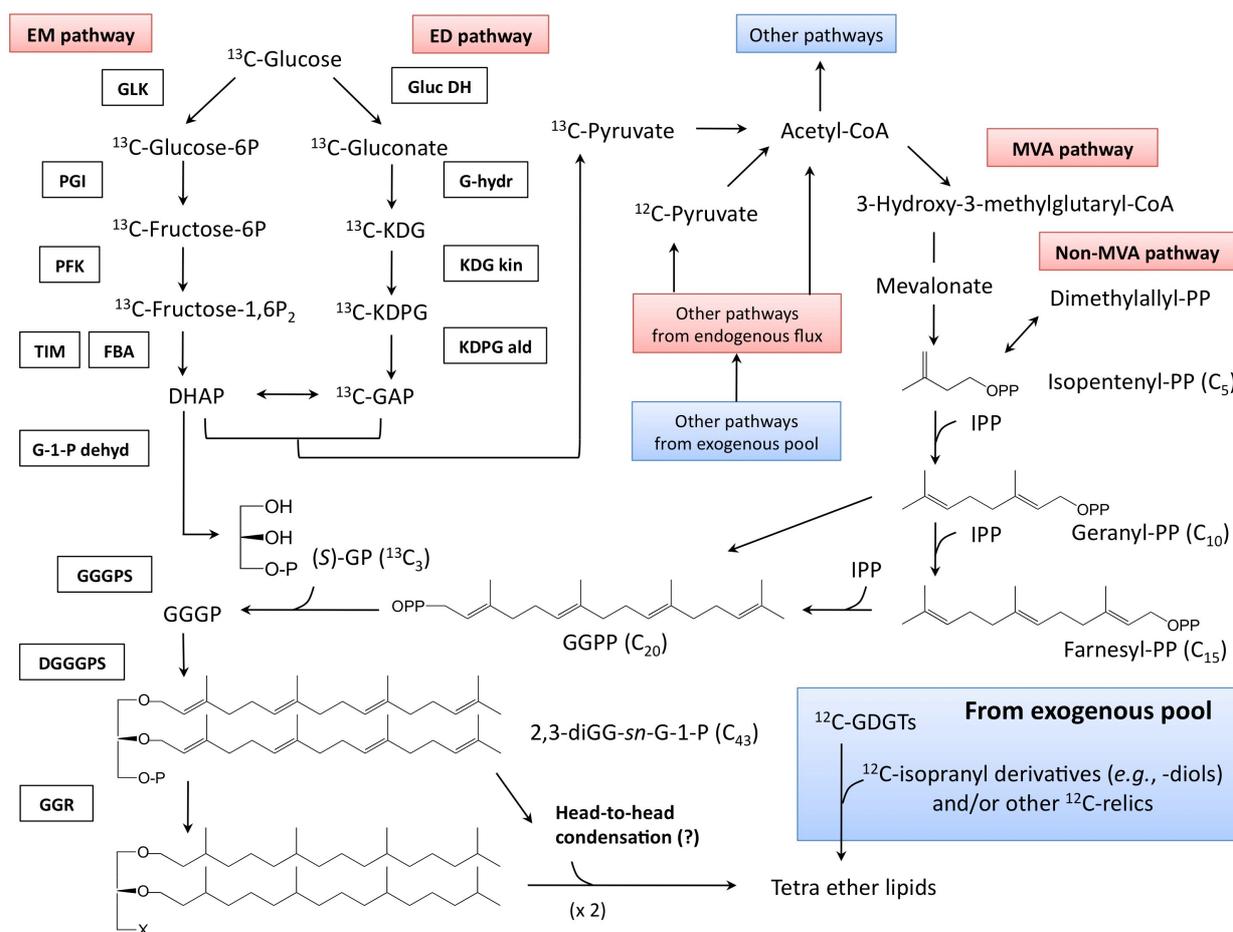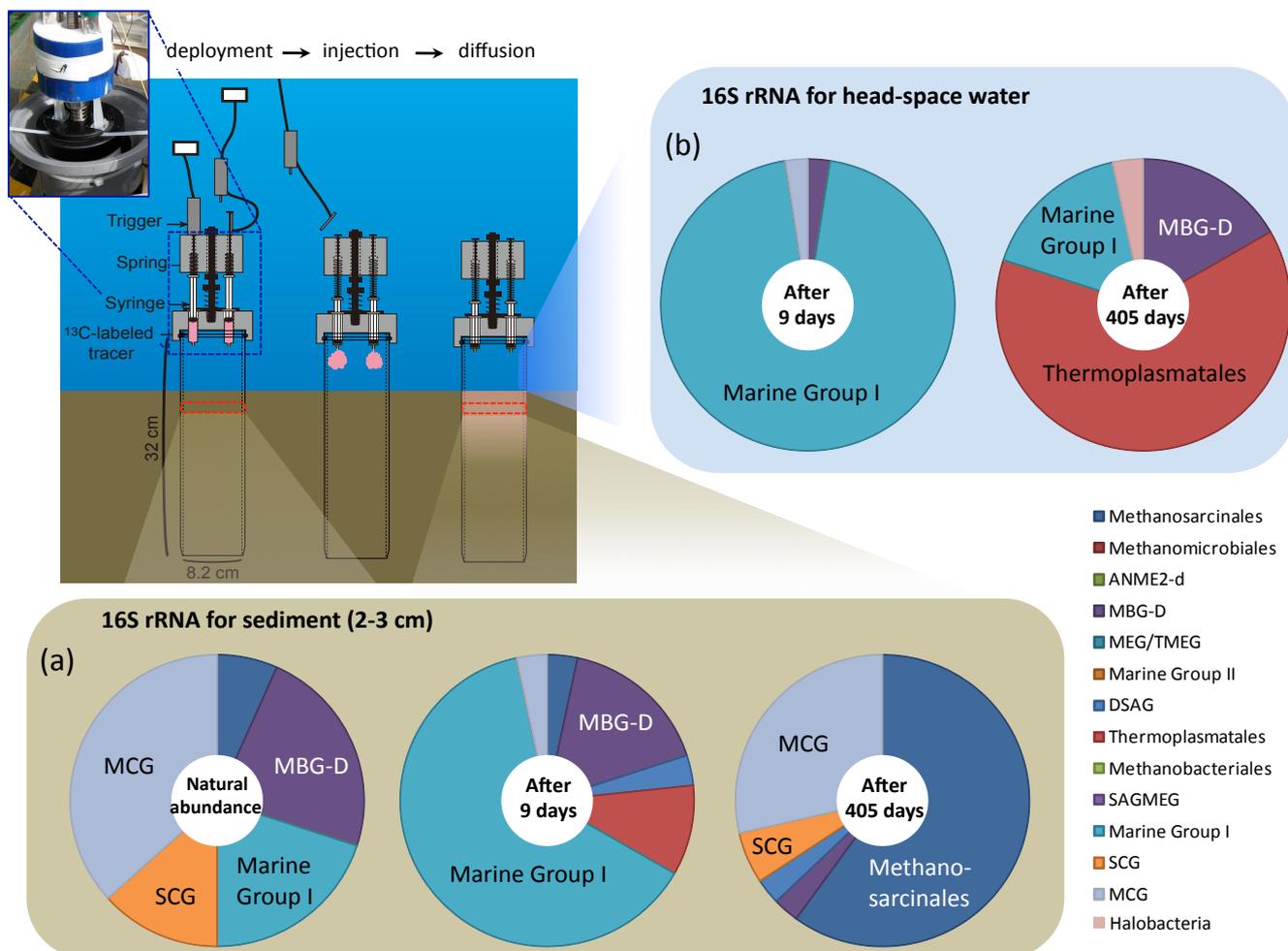
Supplementary Figure 7.

Biosynthesis of core lipids in Archaea for isoprenoid and 2,3-*sn*-glycerol moieties [65-70,74,75]. Red and blue squares stand for endogenous and exogenous processes for benthic archaea, respectively. Abbreviations and enzymes (black squares): EM, Embden-Meyerhof; ED, Entner-Doudoroff; GLK, glucokinase; PGI, phosphoglucose isomerase; PFK, phosphofructokinase; TIM, triosephosphate isomerase; FBA, Fructose-1,6-bisphosphate aldolase; Gluc DH, Glucose dehydrogenase; G-hyd, Gluconate dehydratase; KDG kin, 2-keto-3-deoxygluconate kinase; KDPG ald, 2-keto-3-deoxy-6-phosphogluconate aldolase; G-1-P DH, G-1-P dehydrogenase; GGGPS, 3-*O*-geranylgeranylglyceryl phosphate synthase; DGGGPS, 2,3-di-*O*-geranylgeranylglyceryl phosphate synthase[65]; GGR, geranylgeranyl reductase[66]; IPP, isopentenyl diphosphate; GGPP, geranylgeranyl diphosphate; (*S*)-GP, (*S*)-glyceryl phosphate. X denotes a polar head group. Note that salvage pathway of lipid was observed in *Sulfolobus acidocaldarius*[75].

Supplementary Figure 8.

Schematic design of the *in situ* ^{13}C-tracer experiment using I-K type incubation chambers[17,38,39]. **a**, Phylogenic analysis of the benthic archaeal community, showing natural abundance and *in situ* ^{13}C-tracer experiment, 9 days (G-9) and 405 days (G-405) at mid-depth 2.5 cm. **b,** Phylogenic analysis of head-space water sample for G-9 and G-405. Abbreviations; ANME2-d, Anaerobic oxidation of methane 2-d; MBG-D, Marine Benthic Group D; MEG/TMEG, Miscellaneous Euryarchaeotal Group/Terrestrial Miscellaneous Euryarchaeotal Group; GSAG, Deep-Sea Archaeal Group; SAGMEG, South African Goldmine Euryarchaeotal Groups; MCG, Miscellaneous Crenarchaeotic Group. Marine Group I as well as other phylogenetic affiliations were analyzed using ARB software (AB561312-AB561824; 513 entries).

We conducted 16S rRNA analysis and qPCR for sub-surface and head-space water samples (Fig. 3 and Suppl. Figs. 8&9). We observed distinct increase of benthic archaeal abundance from 10^5-10^7 copies g-sed^{-1}. In contrast, the abundance of archaea in head-space water was much lower than sedimentary archaea for 3-5 orders of magnitude. Considering the structures of the capped upper part of incubator (Suppl. Fig. 8), we concluded that pelagic archaea from water column could not have an infiltration pathway, but distinct archaeal community shift occurred inside of the chamber.

Because the carbon isotopic composition of dissolved inorganic carbon ($\delta^{13}C_{DIC}$) exceeded +4200‰ (Suppl. Fig. 9) in headspace water samples from the G-9 series[48], if the carbon fixation pathway involved the uptake of dissolved inorganic carbon for isoprenoid biosynthesis, the intramolecular carbon isotopic compositions for each isoprenoid should also be ^{13}C-labeled (Ref. 4). Previous studies have investigated the permeability of the outer membrane in Prokaryote[49-57]. The passage of solutes across the channel is limited to small polar molecules, thought to be generally 1000 Da or more[25], through porin protein channels[54,58,59]. Transport models of long-chain fatty acids and other hydrophobic molecules across the outer membrane have been reported using an *E. coli* analog[57]. Furthermore, when *E. coli* is starved of carbon sources, outer membrane porin production responds to the growth rate[56]. As a plausible exogenous compound for our hypothesis regarding archaeal reutilization, free and bound alkyl isoprenoid compounds including biphytanediols have been identified from sediment samples[29,60-62,77]. Our finding of a pronounced heterogeneity in carbon isotopic composition between 2,3-s*n*-glycerol and alkyl isoprenoids indicates that the incorporation pathway from

exogenous alkyl isoprenoid compounds occurred during benthic archaeal growth, presumably for reutilization as endogenous isoprenoid compounds by importing them through the outer membrane. Additional *in-situ* ^{13}C-experiments are needed to validate a hypothesis of recycling pathway to specify the sources of extracellular organic compounds.
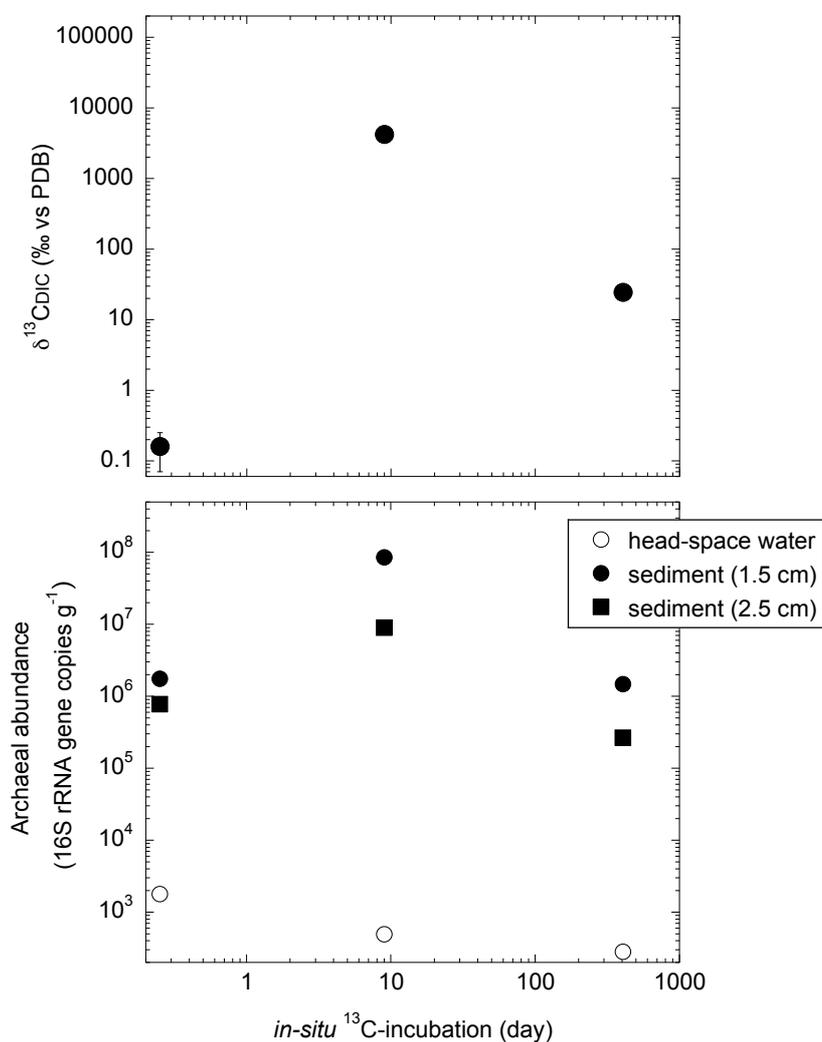
Supplementary Figure 9.

$\delta^{13}C_{DIC}$ **and archaeal abundance by quantitative PCR (qPCR,** *n***=3) for head-space water and sediment samples inside of the incubation chamber.** $\delta^{13}C_{DIC}$ in head-space water were 0.16 ± 0.1‰, 4214.0 ± 51.4‰, 24.4 ± 0.6 ‰ for G-0, G-9, and G-405 samples, respectively. Concentration of extractable archaeal core-lipids (sum of caldarchaeol, GDGT1, GDGT2, GDGT3, Crenarchaeol)[45] for 0 day, 9 days and 405 days in the surfaces were 13.3 ± 4.0 (*n*=3), 14.5 ± 2.1 (*n*=3), 16.8 ± 3.0 μg/dry-sediment (*n*=3), respectively. Archaeol (di-ether) was not significant amount in the present sample.

Supplementary Table 1.

Total organic carbon (TOC, wt%), carbon isotopic composition of bulk sedimentary organic carbon ($\delta^{13}C_{TOC}$), and compound-specific isotope analysis (CSIA) of caldarchaeol and crenarchaeol during the *in situ* tracer experiment for 0 day (G-0), 9 days (G-9) and 405 days (G-405).

	In situ ^{13}C-tracer experiment (G-0)				*In situ* ^{13}C-tracer experiment (G-9)			
	Total organic carbon		CSIA of archaeal lipids		Total organic carbon		CSIA of archaeal lipids	
depth	TOC	$\delta^{13}C_{TOC}$	$\delta^{13}C$caldarchaeol	$\delta^{13}C$crenarchaeol	TOC	$\delta^{13}C_{TOC}$	$\delta^{13}C$caldarchaeol	$\delta^{13}C$crenarchaeol
cm	wt%	‰ vs. PDB	‰ vs. PDB		wt%	‰ vs. PDB	‰ vs. PDB	
0-1	2.1	99.1	-21.4	-21.7	2.3	271.6	45.7	21.9
1-2	2.1	37.3	-	-	2.2	34.4	-9.9	-8.9
2-3	2.2	50.4	-	-	1.7	4.0	-14.5	-12.9
3-4	2.5	-4.0	-	-	1.8	-0.8	-18.4	-14.7
4-5	2.4	-17.5	-23.0	-22.7	2.1	-7.7	-17.2	-14.6
5-7	2.2	-21.4	-	-	1.9	-16.8	-	-
7-10	2.1	-21.4	-	-	2.4	-19.1	-	-
10-15	2.4	-21.2	-	-	2.0	-13.3	-20.7	-18.4
average	2.2 ± 0.2				2.1 ± 0.3			

	In situ ^{13}C-tracer experiment (G-405)			
	Total organic carbon		CSIA of archaeal lipids	
depth	TOC	$\delta^{13}C_{TOC}$	$\delta^{13}C$caldarchaeol	$\delta^{13}C$crenarchaeol
cm	wt%	‰ vs. PDB	‰ vs. PDB	
0-1	1.5	186.5	68.7	132.4
1-2	1.8	20.3	6.2	10.9
2-3	2.6	2.1	-	-
3-4	2.5	-14.4	-	-
4-5	2.5	-17.5	-20.5	-19.8
average	2.2 ± 0.5			

Supplementary Table 2.

Results of carbon isotopic compositions of $\delta^{13}C_{caldarchaeol}$, $\delta^{13}C_{crenarchaeol}$, $\delta^{13}C_{biphytane}$ and $\delta^{13}C_{2,3\text{-}sn\text{-glycerol}}$ during *in situ* ^{13}C-tracer experiments ; 0 days (G-0), 9 days (G-9) and 405 days (G-405).

In situ ^{13}C-tracer experiment (G-405)				*In situ* ^{13}C-tracer experiment (G-405)					
Intramolecular CSIA of caldarchaeol			difference	Intramolecular CSIA of crenarchaeol				difference	
depth cm	$\delta^{13}C_{2,3\text{-}sn\text{-glycerol}}$	$\delta^{13}C_{BP[0]}$	$\Delta\delta^{13}C_{glycrol\text{-}BP[0]}$	$\delta^{13}C_{2,3\text{-}sn\text{-glycerol}}$	$\delta^{13}C_{BP[2]}$	$\delta^{13}C_{BP[3]}$		$\Delta\delta^{13}C_{glycrol\text{-}BP[2]}$	$\Delta\delta^{13}C_{glycrol\text{-}BP[3]}$
	‰ vs. PDB				‰ vs. PDB				
0-1	1278	-22.0 (*n*=2)	1300	2193	-22.2	-22.1	(*n*=2)	2216	2216

In situ ^{13}C-tracer experiment (G-9)				*In situ* ^{13}C-tracer experiment (G-9)					
Intramolecular CSIA of caldarchaeol			difference	Intramolecular CSIA of crenarchaeol				difference	
depth cm	$\delta^{13}C_{2,3\text{-}sn\text{-glycerol}}$	$\delta^{13}C_{BP[0]}$	$\Delta\delta^{13}C_{glycrol\text{-}BP[0]}$	$\delta^{13}C_{2,3\text{-}sn\text{-glycerol}}$	$\delta^{13}C_{BP[2]}$	$\delta^{13}C_{BP[3]}$		$\Delta\delta^{13}C_{glycrol\text{-}BP[2]}$	$\Delta\delta^{13}C_{glycrol\text{-}BP[3]}$
	‰ vs. PDB				‰ vs. PDB				
0-1	889	-17.6 (*n*=2)	907	491	-9.3	-17.3	(*n*=2)	501	509
1-2	110	-18.9 (*n*=2)	129	132	-18.8	-20.1	(*n*=2)	151	152

Supplementary References

31 Okutani, T. & Egawa, K. The first underwater observation on living habitat and thanatocoenoses of Calyptogena soyoae in bathyal depth of Sagami Bay. *Venus* **44**, 285-289 (1985).

32 Urakawa, H., Yoshida, T., Nishimura, M. & Ohwada, K. Characterization of depth-related population variation in microbial communities of a coastal marine sediment using 16S rDNA-based approaches and quinone profiling. *Environ. Microbiol.* **2**, 542-554 (2000).

33 Kitazato, H. *et al.* Long-term monitoring of the sedimentary processes in the central part of Sagami Bay, Japan: rationale, logistics and overview of results. *Prog. Oceanogr.* **57**, 3-16 (2003).

34 Nakatsuka, T. *et al.* Particle dynamics in the deep water column of Sagami Bay, Japan. I: origins of apparent flux of sinking particles. *Prog. Oceanogr.* **57**, 31-45 (2003).

35 Shimanaga, M. & Shirayama, Y. Response of benthic organisms to seasonal change of organic matter deposition in the bathyal Sagami Bay, central Japan. *Oceanol. Acta* **23**, 91-107 (2000).

36 Fujikura, K., Okutani, T. & Maruyama, T. Deep-sea life: biological observations using research submersible. pp. 1-487. Tokai Univ Press. (2008).

37 Fang, J., Shizuka, A., Kato, C. & Schouten, S. Microbial diversity of cold-seep sediments in Sagami Bay, Japan, as determined by 16S rRNA gene and lipid analyses. *FEMS Microbiol. Ecol.* **57**, 429-441 (2006).

38 Nomaki, H. *et al.* Different ingestion patterns of delta ^{13}C-labeled bacteria and algae by deep-sea benthic foraminifera. *Mar. Ecol. Progr. Ser.* **310**, 95-108 (2006).

39 Nomaki, H., *et al.* Degradation of algal lipids by deep-sea benthic foraminifera: An in situ tracer experiment. *Deep Sea Res. –I.* **56**, 1488-1503 (2009).

40 The bathymetric data were acquired during JAMSTEC cruises KR01-10, KR04-03, KR04-09, KR04-13, KR06-04, KR07-01, KR07-11, KY02-01, KY02-11, KY03-11, KY04-08, KY04-11, KY05-06, KY06-01, KY06-03, KY06-11, KY07-05, KY07-14, NT04-00, NT04-ENG, NT06-01, NT06-01, NT06-07, NT06-E01, YK00-05, YK01-05, YK01-11, YK05-07, YK07-06 and YK07-06 (courtesy from each P.I).

41 Boucher, Y., Kamekura, M. & Doolittle, W. Origins and evolution of isoprenoid lipid biosynthesis in archaea. *Mol. Microbiol.* **52**, 515-527 (2004).

42 Nishihara, M., Morii, H. & Koga, Y. Structure determination of a quartet of novel tetraether lipids from *Methanobacterium-Thermoautotrophicum*. *J. Biochem.* **101**, 1007-1015 (1987).

43 Koga, Y., Nishihara, M., Morii, H. & Akagawa-matsushita, M. Ether polar lipids of methanogenic bacteria - structures, comparative aspects, and biosyntheses. *Microbiol. Rev.* **57**, 164-182 (1993).

44 Sinninghe Damste, J. S., Schouten, S., Hopmans, E. C., van Duin, A. C. T. & Geenevasen, J. A. J. Crenarchaeol: the characteristic core glycerol dibiphytanyl glycerol tetraether membrane lipid of cosmopolitan pelagic crenarchaeota. *J. Lipid Res.* **43**, 1641-1651 (2002).

45 Huguet, C. *et al.* An improved method to determine the absolute abundance of glycerol dibiphytanyl glycerol tetraether lipids. *Org. Geochem.* **37**, 1036-1041 (2006).

46 Ohkouchi, N. *et al.* Biogeochemical processes in the saline meromictic Lake Kaiike, Japan: implications from molecular isotopic evidences of photosynthetic pigments. *Environ. Microbiol.* **7**, 1009-1016 (2005).

47 Ogawa, O.N., Nagata, T., Kitazato, H. & Ohkouchi, N. Ultra sensitive elemental analyzer/isotope ratio mass spectrometer for stable nitrogen and carbon isotope analyses. *Earth, Life, and Isotopes* (edited by N. Ohkouchi, I. Tayasu, and K. Koba), Kyoto University Press. 339-353 (2010).

48 Nomaki, H., Ogawa, O. N., Ohkouchi, N. & Kitazato, H. Particulate versus dissolved organic matter uptake by deep-sea benthic foraminifera revealed by *in situ* ^{13}C-labeling experiments. Japan Geoscience Union meeting. B102-P011 (2008).

49 Benz, R., Schmid, A. & Hancock, R. Ion selectivity of gram-negative bacterial porins. *J. bacterial.* **162**, 722-727 (1985).

50 Kumar, G. & Black, P. Bacterial long-chain fatty acid transport. *J. Biol. Chem.* **268**, 15469-15476 (1993).

51 Phale, P. *et al.* Voltage gating of *Escherichia coli* porin channels: role of the constriction loop. *Proc. Natl Acad. Sci. USA*. **94**, 6741-6745 (1997).

52 Le Dain, A., Saint, N., Kloda, A., Ghazi, A. & Martinac, B. Mechanosensitive ion channels of the archaeon *Haloferax volcanii*. *J. Biol. Chem.* **273**, 12116-12119 (1998).

53 Kleinfeld, A. Lipid phase fatty acid flip-flop, is it fast enough for cellular transport ? *J. Memb. Biol.* **175**, 79-86 (2000).

54 Kloda, A. & Martinac, B. Molecular identification of a mechanosensitive channel in archaea. *Biophys. J.* **80**, 229-240 (2001).

55 Perozo, E. & Rees, D. Structure and mechanism in prokaryotic mechanosensitive channels. *Curr. opinion structural biol.* **13**, 432-442 (2003).

56 Nikaido, H. Molecular basis of bacterial outer membrane permeability-revisited. *Microbiol. Mol. Biol. Rev.* **67**, 593-656 (2003).

57 Van den Berg, B., Black, P., Clemons, W. & Rapoport, T. Crystal structure of the long-chain fatty acid transporter FadL. *Science* **304**, 1506-1509 (2004).

58 Voet, D. & Voet, G. J. Biochemistry -third edition-, John Wiley & Sons Inc. (2004).

59 Madigan, T. M., Martinko, M. J. & Parker, J., Brock biology of Microorganisms –nine edition-, Prentice hall Inc. (2003).

60 Pancost, R., Sinninghe Damste, J., de Lint, S., van der Maarel, M. & Gottschal, J. Biomarker evidence for widespread anaerobic methane oxidation in Mediterranean sediments by a consortium of methanogenic archaea and bacteria. *Appl. Environ. Microbiol.* **66**, 1126-1132 (2000).

61 Teske, A. *et al.* Microbial diversity of hydrothermal sediments in the Guaymas Basin: evidence for anaerobic methanotrophic communities. *Appl. Environ. Microbiol.* **68**, 1994-2007 (2002).

62 Hinrichs, K. & Boetius, A. The anaerobic oxidation of methane: new insights in microbial ecology and biogeochemistry. *Ocean Margin Systems*. Springer-Verlag Berlin Heidelberg, 457-477 (2002).

63 Turich, C. *et al.* Lipids of marine Archaea: Patterns and provenance in the water-column and sediments. *Geochim. Cosmochim. Acta* **71**, 3272-3291 (2007).

64 Chikaraishi, Y. & Naraoka, H. δ^{13}C and δD relationships among three *n*-alkyl compound classes (*n*-alkanoic acid, *n*-alkane and *n*-alkanol) of terrestrial higher plants. *Org. Geochem.* **38**, 198-215 (2007).

65 Hemmi, H., Shibuya, K., Takahashi, Y., Nakayama, T. & Nishino, T. (*S*)-2,3-Di-*O*-geranylgeranylglyceryl phosphate synthase from the thermoacidophilic Archaeon *Sulfolobus solfataricus*. *J. Biol. Chem.* **279**, 50197-50203 (2004).

66 Murakami, M. *et al.* Geranylgeranyl reductase involved in the biosynthesis of archaeal membrane lipids in the hyperthermophilic archaeon *Archaeoglobus fulgidus*. *FEBS J.* **274**, 805-814 (2007).

67 Morii, H., Nishihara, M. & Koga, Y. CTP: 2, 3-di-*O*-geranylgeranyl-*sn*-glycero-1-phosphate cytidyl transferase in the methanogenic archaeon *Methanothermobacter thermoautotrophicus*. *J. Biol. Chem.* **275**, 36568-36574 (2000).

68 Zhang, D. & Poulter, C. Biosynthesis of archaebacterial lipids in *Halobacterium halobium* and *Methanobacterium thermoautotrophicum. J. Org. Chem.* **58**, 3919-3922 (1993).

69 Nemoto, N., Shida, Y., Shimada, H., Oshima, T. & Yamagishi, A. Characterization of the precursor of tetraether lipid biosynthesis in the thermoacidophilic archaeon *Thermoplasma acidophilum. Extremophiles* **7**, 235-243 (2003).

70 Nishihara, M., Yamazaki, T., Oshima, T. & Koga, Y. *sn*-Glycerol-1-Phosphate- forming activities in Archaea: separation of Archaeal phospholipid biosynthesis and glycerol catabolism by glycerophosphate enantiomers. *J. Bacteriol.* **181**, 1330-1333 (1999).

71 Morono, Y., Terada, T., Masui, N. & Inagaki, F. Discriminative detection and enumeration of microbial life in marine subsurface sediments. *ISME J.* **3**, 503-511 (2009).

72 Kashiyama, Y. *et al.* Evidence of global chlorophyll-*d. Science* **321**, 658-658 (2008).

73 Flemings, P.B., Behrmann, J.H., John, C.M. & the Expedition 308 Scientists, *Proc. IODP, 308*: College Station TX (Integrated Ocean Drilling Program Management International, Inc.). doi:10.2204/iodp.proc.308.2006 (2006).

74 Nicolaus, B. *et al.* Calditol tetraether lipids of the archaebacterium *Sulfolobus solfataricus. Biochem. J.* **266**, 785-791 (1990).

75 Ohnuma, S., Watanabe, M. & Nishino, T. Identification and characterization of geranylgeraniol kinase and geranylgeranyl phosphate kinase from the Archaebacterium *Sulfolobus acidocaldariu. J. Biochem.* **119**, 541-547 (1996).

76 Lin, Y.S. In vitro study of microbial carbon cycling in subseafloor sediments. PhD Thesis, Univ Bremen. pp.1-151 (2009).

77 Saito, H. & Suzuki, N. Distribution of acyclic and cyclic biphytanediols in recent marine sediments from IODP Site C0001, Nankai Trough. *Org. Geochem.* **41**, 1001-1004 (2010).